J Therm Anal Calorim (2013) 111:145–154
DOI 10.1007/s10973-012-2241-6

Catalytic oxidation of CO on platinum

Thermochemical approach

Boris V. L'vov · Andrew K. Galwey

Received: 14 November 2011 / Accepted: 18 January 2012 / Published online: 19 February 2012

Abstract Using concepts recently developed in thermal decompositions of solids and reduction of bulk oxides by gases and (re)analysis of experimental literature data, a novel mechanism for the catalytic oxidation of CO by PtO_2 is proposed. Instead of the conventional Mars–van Krevelen scheme, the reactions proposed are: $PtO_2(s) + 2CO \longleftrightarrow Pt(g) + 2CO_2$ and $Pt(g) + O_2 \longleftrightarrow PtO_2(g) \rightarrow PtO_2(s)$. The first reaction determines the kinetics of CO oxidation and the second determines the kinetics of restoration of the PtO_2 layer. Thermochemical consideration of the kinetic features of this model, based on Langmuir's quasi-equilibrium equations for evaporation of simple substances, allowed calculation of the reaction enthalpy and the absolute rate of CO oxidation. These results are in good agreement with experimental data. The proposed mechanism explains the origin of the surface-retexturing effect, the limited loss of Pt metal from the catalyst, the mechanism of PtO_2 regeneration by oxygen, the strong effect of CO_2 in reducing the CO oxidation rate and the three-fold variation of the Arrhenius E parameter with temperature.

Keywords Catalytic CO oxidation on Pt · Congruent decomposition of PtO_2 · Enthalpy for CO oxidation on Pt catalyst · Limited Pt losses during CO oxidation · Mechanism of PtO_2-restoration in CO oxidation · Thermochemistry of heterogeneous catalysis

B. V. L'vov
Department of Analytical Chemistry, St. Petersburg State Polytechnic University, St. Petersburg, Russia 195251

A. K. Galwey (✉)
Department of Chemistry, Rhodes University, Grahamstown 6140, South Africa
e-mail: aandk.galwey@talktalk.net

Introduction

Ninety years after Langmuir's first, pioneering, study of the catalytic oxidation of carbon monoxide on platinum ($2CO + O_2 = 2CO_2$) [1, 2], this reaction continues to be an important topic of active research. A main reason is that this has been selected as a representative reaction in studies directed toward reducing polluting emissions, including CO, from internal combustion engines.

Within the extended literature of heterogeneous catalysis, including CO oxidation on platinum group metals (PGM), three alternative, and well-known, mechanistic models are used to represent behavior. These are the Langmuir–Hinshelwood mechanism (LH) [2–4], involving interactions between adsorbed species on an active surface, the Eley–Rideal mechanism (ER), 1940 [5, 6], where (LH-type) adsorbed species react with gaseous molecules, and the Mars–van Krevelen mechanism (MvK) 1954 [7] where the desorbed products contain species derived from the catalyst. These three mechanisms show the progressive development of the theory from pure-adsorption (LH) to partly adsorption (ER) models, for reactions on rigid 'promoting' surfaces, to involvement (MvK) by a chemically active substrate/intermediate. Nevertheless, the oldest, and most familiar, LH mechanism maintains its preeminence as the preferred approach to the interpretation of experimental results. According to Scopus (The largest citation database of peer-reviewed literature), references in reports of all heterogeneous catalytic reactions for the 50 years, 1960–2010, cited the LH, ER, and MvK mechanisms ca. 1250, 500, and 190 times, respectively.

According to the MvK mechanism, CO oxidation on PtO_2 can be represented by the following steps:

$$PtO_2(s) + 2CO \leftrightarrow Pt(s) + 2CO_2 \quad (1)$$

$$Pt(s) + O_2 \leftrightarrow PtO_2(s) \quad (2)$$

First, in a high partial pressure of O_2 and at elevated temperatures, the metal is oxidized. After formation of a surface layer of platinum oxide, gaseous CO molecules are adsorbed and react with oxygen in the PtO_2 to produce CO_2. The resulting oxide vacancies in the PtO_2 layer are refilled rapidly from the gaseous O_2 present. However, the strengths and weaknesses of these mechanisms have not been adequately appraised. Unresolved problems include: the significance of the Arrhenius parameter E, the retexturing of Pt surfaces during CO oxidation and the mechanism of continuous regeneration of the PtO_2 active surface layer.

The goal of this study is to develop a mechanism of heterogeneous catalysis that shares some features of the MvK model but removes (partly or totally) the obstacles identified above. Of the two states (steps), considered in the alternation of CO oxidation on Pt and PtO_2 during oscillations, and interpreted [8] by the 'switching' between two different mechanisms (LH and MvK), the present consideration will be directed only toward the state related to the oxidation of CO on PtO_2 in high (around atmospheric) pressures of CO and O_2. This is achieved here by using concepts of the thermochemical approach, which have recently been developed, and successfully applied, in the adjacent fields of heterogeneous reactions: the thermal decompositions of solids and the reduction of bulk oxides by gases.

Theoretical

This section introduces concepts from thermochemical theory, which have never previously been applied in the kinetic and mechanistic investigations of heterogeneous catalysis (Table 1).

Methodology of kinetic studies

Two principal approaches have been used in the development of theory applicable to heterogeneous rate processes. These derive from the work of Arrhenius (the kinetic and mechanistic approach) and of Langmuir (the thermochemical approach). The former is widely employed, being conventionally used in studies of reactions of, and on, solids and is based on Arrhenius' equation:

$$k = A\exp(-E/RT) \quad (3)$$

The thermochemical approach, formulated by L'vov et al. [9–20] 30 years ago, uses Langmuir quasi-equilibrium equations for the evaporation of a simple substance (such as a metal) in vacuum or in an inert gas:

Table 1 Main differences between the conventional and the thermochemical approaches to kinetic and mechanistic analysis of thermal decompositions of solids, solid oxide reductions, and heterogeneous catalytic reactions

Section of theory	Conventional approach	Thermochemical approach
Mechanism	Incongruent decomposition of oxides of low-volatile metals (solid → solid)	Congruent decomposition of oxides to gaseous products with rapid subsequent condensation of super-saturated vapor of low-volatile metals (solid → gas → solid)
Kinetics	Arrhenius kinetic equation	Langmuir quasi-equilibrium equations for vaporization in vacuum and in a foreign gas, including the concepts of equimolar and isobaric reduction modes

$$J = MP/(2\pi MRT)^{1/2} \quad (4)$$

$$J = MDP/(zRT) \quad (5)$$

$$J = MDP/(rRT) \quad (6)$$

Here J is the absolute evaporation rate (kg m^{-2} s^{-1}), M is molar mass, D is the diffusion coefficient of the vapor in a reactor atmosphere, z is the distance from the vaporization surface to the sink, where the vapor concentration is zero, and r is the radius of a spherical particle of the substance. Eq. 4, for vacuum, was derived by Hertz, Knudsen, and Langmuir; the diffusion Eqs. 5 and 6 were developed by Langmuir (see details in [15]). All absolute vaporization rates J are directly proportional to the equilibrium vapor pressures P of the substance.

The Langmuir vaporization equations were derived by considering the equilibrium that exists between the two simultaneous reverse processes (vaporization and condensation) during the decomposition reaction. The partial pressures of gaseous products:

$$A_aB_b(s) \leftrightarrow aA(g) + bB(g) \quad (7)$$

under steady-state conditions are related through the equilibrium constant:

$$K_P = (P_A)^a(P_B)^b \quad (8)$$

This opens the opportunity to use thermodynamic concepts and thermochemical data for the quantitative analysis and interpretation of the kinetics of decompositions and reductions of solids [15]. The advantages of using the Langmuir equations rather than the Arrhenius equation consist not only in the introduction of the chemical-equilibrium concept into heterogeneous kinetics but also in the thermodynamic substantiation of the exponential dependence of

reaction rate on temperature. Instead of the active-molecule hypothesis introduced by Arrhenius, this feature is interpreted as thermodynamic justification of the impact of temperature on the equilibrium constant.

The mechanism of congruent dissociative vaporization

Thermal decomposition of a solid (or liquid) reactant, AB, can be described by the alternative processes: congruent dissociative vaporization (CDV) to gaseous products A(g) and B(g), only:

$$AB(s/l) \leftrightarrow A(g) + B(g) \quad (9)$$

or by incongruent dissociative vaporization to a solid product A(s) and a gaseous product B(g) by:

$$AB(s/l) \leftrightarrow A(s) + B(g) \quad (10)$$

The existence of these two fundamentally different schemes of decomposition is recognized and is generally accepted without evoking any objections or doubt. However, in contrast to the first scheme, the second appears, on closer examination, to be questionable for the following reasons [15]. Equation 10 requires a recrystallization step: the structure of the solid product, A(s), is different from that of the solid reactant AB(s). In addition, the products undergo retexturing whereby the residual components are transformed into product conglomerates, composed of separated nano-particles. This finely divided residue is effectively 'transparent' to the exhaust flow of evolved gaseous products. Furthermore, in more complicated reactions, two, or more, solid products may be formed as separated particles of different phases. An example is the decomposition of talc, ($MgO{\cdot}4SiO_2{\cdot}H_2O$), which results in the simultaneous production of enstatite ($MgSiO_3$) and an amorphous form of SiO_2. It is difficult to imagine how a solid reactant can be transformed into one or more solid product(s), having different crystal structures from that of the reactant, without an intermediate stage involving a change (or changes) in the state of aggregation (through melting or evaporation).

The pattern of behavior observed in these reactions is much more reasonably explained on the assumption that solid products form as a result of collisions and condensations of low-volatility particles (atoms and molecules) generated in the gaseous phase through decomposition by the congruent dissociative vaporization mechanism, represented by:

$$AB(s/l) \leftrightarrow A(g) + B(g) \rightarrow A(s) + B(g) \quad (11)$$

This is conveniently abbreviated to:

$$AB(s/l) \leftrightarrow A(g)_{\downarrow} + B(g) \quad (12)$$

The assumptions underlying this approach, in its most recent form, are summarized as follows [15].

(i) The primary step in decomposition is the congruent dissociative evaporation of reactant. Where products of low-volatility form, this is followed by their condensation step.

(ii) The energy evolved by the condensation of low-volatility product within a reaction interface is distributed in approximately equal proportions between the reactant and product solid phases. That part of the energy directly transferred to the reactant promotes decomposition (as part of the enthalpy change) and manifests itself in the appearance of induction and acceleration periods (the effect of autocatalysis). For reactions proceeding on an open surface, the condensation energy is released/distributed in the immediate vicinity of the surface.

These assumptions have been confirmed by reliable experimental observations, made during the last 30 years by direct quadrupole mass spectrometric (QMS) analyses of the primary gaseous products evolved during thermal decompositions of microgram masses of several metal nitrates [11–14]. Further extensive support has been given by thermogravimetric kinetic studies [15–20] of the decompositions of a huge number of diverse solid reactants: oxides, nitrides, azides, hydroxides, clays, hydrates, nitrates, sulfates, carbonates, oxalates, and permanganates.

The mechanism of congruent dissociative reduction of bulk oxides

The thermochemical approach, previously used to interpret the kinetics and mechanisms of solid-state thermal decompositions [15] was recently extended, for the first time, to analyze rate data for the reduction of a metal oxide (NiO) by hydrogen [21]. Our analysis [21] showed that the thermochemical approach quantitatively accounts for the kinetic characteristics of the selected reduction reaction. Furthermore, this theoretical analysis explains kinetic features not previously recognized. In particular, the dependencies of reduction rates on hydrogen pressure, in the absence and in the presence of H_2O vapor, are explained. Moreover, the more than two-fold decrease of the E parameter with the extent of reaction, α, and also, at high α, the systematic increase of E with temperature has been quantitatively interpreted.

In contrast with the thermal decompositions of (many) solids and the reductions of bulk metal oxides, the congruent dissociative reduction of the PtO_2 sub-monolayer, participating in the catalytic oxidation of CO by Pt, forms no reaction interface between two solid phases. This is supported by the absence of the induction and acceleration periods in the development of catalytic oxidation. Consequently, energy transfer to PtO_2 from low-volatility

product condensation is also absent. This significantly simplifies and improves reliability of the kinetic calculations. Besides, this accounts for the much greater thermal stability of the PtO_2 film, when compared with that of bulk PtO_2. This unexpected behavior was noted and investigated by Shumbera et al. [22], who concluded that "the extra stability is difficult to explain by considering only the thermodynamics of oxide particle or thin film formation". The mechanism of congruent dissociative reduction has enabled this difference to be interpreted quantitatively [21].

Equimolar and isobaric reaction modes

It is important to point out that, in thermal decompositions of solids and in reductions of solid reactants by gases, two different reaction modes (regimes) exist: equimolar and isobaric. These alternative types of kinetic behaviors are distinguished in the following examples. We consider first the reduction of the oxide of a volatile metal (e.g., Cd) by a gas (e.g., CO):

$$MO(s) + CO \leftrightarrow M(g) + CO_2 \tag{13}$$

The equimolar mode (e) refers to reaction in the absence of excess of gaseous product (CO_2), and the isobaric mode (i) in its excess. These different reaction modes were distinguished more than 25 years ago [10], but nobody, except L'vov, has recognized this important kinetic distinction or its consequences. When a gaseous product, here CO_2, is present in the reaction zone, the equilibrium constant is:

$$K_P = P_{\mathrm{M}}^{\mathrm{int}}(P_{\mathrm{CO_2}}^{\mathrm{int}} + P_{\mathrm{CO_2}}^{\mathrm{ext}})/P_{\mathrm{CO}} \tag{14}$$

where $P_{\mathrm{M}}^{\mathrm{int}}$ and $P_{\mathrm{CO_2}}^{\mathrm{int}}$ are equilibrium partial pressures of the metal and CO_2, determined by the reaction itself (internal), and $P_{\mathrm{CO_2}}^{\mathrm{ext}}$ is an externally introduced (constant) partial pressure of CO_2. Under the condition $P_{\mathrm{CO_2}}^{\mathrm{int}} = P_{\mathrm{M}}^{\mathrm{int}} > P_{\mathrm{CO_2}}^{\mathrm{ext}}$, Eq. 14, for the equimolar mode, is:

$$K_P^{\mathrm{e}} = (P_{\mathrm{CO_2}}^{\mathrm{int}})^2/P_{\mathrm{CO}} \tag{15}$$

and, for the isobaric mode, when $P_{\mathrm{M}}^{\mathrm{int}} < P_{\mathrm{CO_2}}^{\mathrm{ext}}$, is:

$$K_P^{\mathrm{i}} = P_{\mathrm{CO_2}}^{\mathrm{int}} \times P_{\mathrm{CO_2}}^{\mathrm{ext}}/P_{\mathrm{CO}} \tag{16}$$

From Eqs. 4–6 and 13–16 we obtain two different relationships for the absolute rates of reduction in equimolar and in isobaric modes:

$$J^{\mathrm{e}} \propto P_{\mathrm{CO_2}}^{\mathrm{int}} = (K_P^{\mathrm{e}} \times P_{\mathrm{CO}})^{1/2} \tag{17}$$

$$J^{\mathrm{i}} \propto P_{\mathrm{CO_2}}^{\mathrm{int}} = K_P^{\mathrm{i}} \times P_{\mathrm{CO}}/P_{\mathrm{CO_2}}^{\mathrm{ext}} \tag{18}$$

For reduction reactions having more complicated stoichiometry, e.g.:

$$M_aO_b(s) + bCO \leftrightarrow aM(g) + bCO_2 \tag{19}$$

the following important conclusions have been deduced [15].

(i) The value of the molar enthalpy, $\Delta_r H_T^\circ/a$, for decomposition in the isobaric mode is independent of the partial pressure of the excess gaseous product in the system, i.e., for any $P_{\mathrm{CO_2}}^{\mathrm{ext}}$ magnitude with $P_{\mathrm{CO_2}}^{\mathrm{ext}} > P_{\mathrm{CO_2}}^{\mathrm{int}}$:

$$\Delta_r H_T^\circ/a = \mathrm{const} \tag{20}$$

(ii) The decomposition rate in the isobaric mode, $J_{\mathrm{CO_2}}^{\mathrm{i}}$, other factors being equal, is inversely related to the magnitude $\left(P_{\mathrm{CO_2}}^{\mathrm{ext}}\right)^{b/a}$, i.e.,

$$J_{\mathrm{CO_2}}^{\mathrm{i}} \propto \left(P_{\mathrm{CO_2}}^{\mathrm{ext}}\right)^{-b/a} \tag{21}$$

(iii) The ratio of the molar enthalpies (and molar entropies) for the isobaric and the equimolar decomposition modes, irrespective of the actual decomposition conditions (vacuum or foreign gas environment), is equal to $(a + b)/a$. E.g., for the reduction of PtO_2 by CO it is predicted that this ratio is 3.

Chemical model for the catalytic oxidation of CO by platinum

The chemical model proposed here for the catalytic oxidation of CO by platinum is based on the important concepts developed from the studies described and cited above. The mechanistic feature includes the congruent reduction of PtO_2 catalyst with the release of gaseous Pt and CO_2. This means that instead of the conventional MvK scheme, the two reactions now proposed are seriously modified forms of Schemes 1 and 2:

$$PtO_2(s) + 2CO \leftrightarrow Pt(g) + 2CO_2 \tag{22}$$

$$Pt(g) + O_2 \leftrightarrow PtO_2(g) \rightarrow PtO_2(s) \tag{23}$$

The first reaction determines the kinetics of CO oxidation, and the second reaction determines the kinetics of regeneration of the PtO_2 layer (Fig. 1). In developing this scheme, we took into account that PtO_2 decomposes to Pt(g) and 2O [23].

It is necessary to assume, that the reactions represented by (22) and (23) take place in the immediate vicinity of the catalyst surface and that the losses of volatilized Pt from the reaction zone are very limited or, as is commonly believed, absent. This statement (assumption) is considered further below ('Physical model' section).

The rate of direct oxidation of solid Pt(s) by O_2 to solid PtO_2(s) is slow. Ackermann's [24] thorough experiments

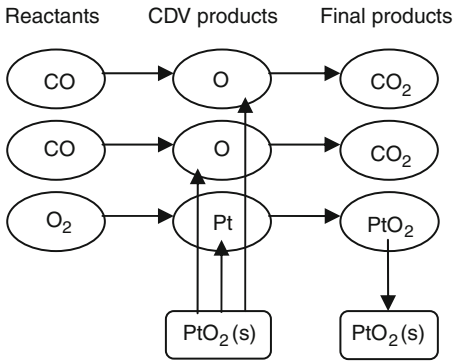

Fig. 1 The chemical model for the catalytic oxidation of CO over PtO_2. Reaction $PtO_2(s) + 2CO \leftrightarrow Pt(g) + 2CO_2$ determines the kinetics of CO oxidation. Reaction $Pt(g) + O_2 \leftrightarrow PtO_2(g) \rightarrow PtO_2(s)$ determines the kinetics of PtO_2 restoration

confirmed conclusively that the rate of this reaction (Pt metal oxidation) is about 2–3 orders of magnitude slower than the maximum rate of CO oxidation on PtO_2.

Reaction enthalpy, $\Delta_r H_T^\circ$, and the equilibrium constant:

$$K_P = P_{Pt} \times P_{CO_2}^2 / P_{CO}^2 \quad (24)$$

for the main reaction (22) are easily calculated at selected temperatures (400, 500, and 600 K) using known values of the thermodynamic functions [25, 26] (the enthalpies of formation, $\Delta_f H_T^\circ$, and entropies, S_T°) for all the components of reaction (22). The results of these calculations are presented in Tables 2 and 3. The enthalpy of this reaction between 500 and 600 K is close to 128 kJ mol^{-1} and K_P increases from 2.3×10^{-6} bar at 500 K to 4.2×10^{-4} bar at 600 K. The reaction enthalpy agrees with the value of Arrhenius parameter, within experimental error. It is shown below that the average magnitude of E is 116 ± 12 kJ mol^{-1}. Note that the reliability of the tabulated value of $\Delta_f H_{298}^\circ$ for $PtO_2(s)$, used in our calculations, is very low (–134 ± 42 kJ mol^{-1} [25]). This is attributable to the few (only two) publications concerned with determination of the enthalpy of PtO_2 formation.

Another important conclusion follows from the calculated equilibrium constant, K_P, for the first step in reaction (23):

$$K_P = P_{PtO_2} / (P_{Pt} \times P_{O_2}) \quad (25)$$

The ratio of gaseous PtO_2 molecules to free Pt atoms is given by:

$$P_{PtO_2} / P_{Pt} = K_P \times P_{O_2} \quad (26)$$

From values of the thermodynamic functions in Tables 2 and 3, we calculate P_{PtO_2}/P_{Pt} ratios at $P_{O_2} = 1$bar and $T = 500$ K and 600 K as 10^{34} and 10^{27}. It follows that virtually all the platinum in the gaseous phase under these quasi-equilibrium conditions is in the form of PtO_2 molecules.

Physical model for the catalytic oxidation of CO by platinum

The physical model is based on simplified consideration of diffusion fluxes of the products (CO_2, Pt, and PtO_2, after Pt oxidation by O_2) of CO oxidation on a catalyst surface of length L in a laminar reactant (CO and O_2) flow, U, parallel to the catalyst plane [27]. The most important innovation in this proposed model is consideration of the role of the gaseous PtO_2, produced by reaction of free Pt atoms with the gaseous oxygen present. PtO_2 molecules are formed close to the catalyst surface, within the mean free path ($\lambda \approx 10^{-7}$–10^{-5} m), and their subsequent fate is determined by simultaneous diffusions in opposite directions: toward the, PtO_2 coated, catalyst surface and outwards across the boundary layer (thickness, δ). In the former case, they condense, replenishing the PtO_2 layer depleted through its consumption in the process of CO oxidation. Consequently, platinum undergoes a reaction cycle, in which a major proportion (as shown below) of the gaseous PtO_2 molecules condense and regenerate the PtO_2 layer on the catalyst surface. However, a very small amount of volatilized Pt is lost by diffusion of PtO_2 beyond the boundary layer. To estimate this outward diffusive loss of PtO_2 across the boundary layer, we need to know the thickness of the boundary layer [27]. Precise evaluation of δ is practically impossible due to lack of quantitative information about the magnitudes of U and L in the relevant catalytic studies. Therefore, we have estimated its value from the experimental magnitude of z in Eq. 5, using this equation as applied to absolute rates of CO oxidation and believing that $\delta = z$.

After changing the molar mass by the Avogadro constant, N_A, in Eq. 5 we have:

$$z = N_A D P / (J R T) \quad (27)$$

The temperature dependence of D, the diffusion coefficient, was evaluated from:

$$D = D_0 (T/273)^n \quad (28)$$

The value of P was calculated from Eq. 24, taking into account that at $P = P_{CO_2} = P_{Pt}$

$$P = (K_P \times P_{CO}^2)^{1/3} \quad (29)$$

It is shown below (see "Absolute rates of CO oxidation on Pt" section) that the experimentally measured values of J at 500–600 K are in the range 2×10^{20}–7×10^{21} molecules m^{-2} s^{-1}, so that the z parameter, calculated from Eq. 27, varies from 53 to 11 mm. Under low pressure conditions (24 Torr), these values are reasonable.

Now we can estimate the distribution of PtO_2 diffusion flows, inwards, toward the catalyst surface and outwards to

Table 2 Enthalpy change for reaction (22): $PtO_2(s) + 2CO(g) = Pt(g) + 2CO_2(g)$

T/K	$\Delta_f H_T^\circ$/kJ/mol							$\Delta_r H_T^\circ$/kJ/mol
	Pt(s)	Pt(g)	CO_2	CO	$PtO_2(s)$	$PtO_2(g)$	O_2	
400	2.7	567.4	–389.5	–107.6	–127.0	175.8	3.0	130.5
500	5.3	570.1	–385.2	–104.6	–120.0	181.1	6.1	128.8
600	8.1	572.8	–380.6	–101.6	–112.8	186.5	9.2	127.5

Primary $\Delta_f H_T^\circ$ data from [25, 26]

Table 3 Entropy change ΔS_T° and equilibrium constant K_P for reaction (22): $PtO_2(s) + 2CO(g) = Pt(g) + 2CO_2(g)$

T/K	S_T°/J/mol K							ΔS_T°/J/mol K	$\ln K_P$	K_P/bar
	Pt(s)	Pt(g)	CO_2	CO	$PtO_2(s)$	$PtO_2(g)$	O_2			
400	49.2	200.1	225.2	206.1	84.3	274.0	213.8	153.9	–20.7	1.0×10^{-9}
500	55.2	205.5	234.8	212.7	99.8	285.8	220.6	149.8	–13.0	2.3×10^{-6}
600	60.2	211.0	243.2	218.2	112.9	295.8	226.3	148.0	–7.8	4.2×10^{-4}

Primary S_T° data from [25, 26]

the boundary layer edge (J_{PtO_2}). Comparison of the values of λ and z, show that the concentration gradient toward the catalyst surface is 3–4 orders of magnitude greater than in the opposite direction. Taking into account the additional difference between CO_2 and PtO_2 molecules in stoichiometry and diffusion coefficients, the rate of outward loss of PtO_2 from the boundary layer should be about 4–5 orders of magnitude smaller than that of CO_2. We emphasize that the above estimations are only tentative and require further investigation.

Data for CO_2 and PtO_2 evolution from the boundary layer (J_{CO_2} and J_{PtO_2}) are presented in Table 4. The last column shows that below 600 K, under conditions that realistically apply in laboratory experiments, the rate of Pt (metal) removal (J_{Pt}) does not exceed about 1 μg cm^{-2} min^{-1}. Such small losses have not been noticed in such experiments and therefore not investigated. This explains the widespread belief that this catalytic reaction is not accompanied by metal loss through volatilization.

Results and discussion

The Arrhenius parameter E

The Arrhenius parameter E (Eq. 3) might reasonably be regarded as the 'most popular' parameter in kinetic studies of catalytic reactions. However, in contrast with rate measurements in other fields, including homogeneous reactions and thermo-analytical studies of heterogeneous reactions, this parameter is rarely used as evidence for interpretation of the mechanisms of these chemical processes. More usually, E values are used to confirm the correlation of reported results with other studies or to demonstrate inexplicable (unpredicted) impacts of experimental conditions (e.g., temperature range, size of catalyst particle, type of substrate, etc.) on kinetic behavior. Table 5 summarizes reported values of the E parameter determined for CO oxidation on various forms of Pt catalysts (48–172 kJ mol^{-1}) measured over three decades, 1978–2010 [28–47]. Also included is the

Table 4 Oxidation rates of CO on Pt (J_{CO_2}) and diffusional losses of PtO_2 (J_{PtO_2}) and Pt (J_{Pt}) at selected temperatures

T/K	K_P/bar[a]	P_{CO_2}/bar[b]	D_{CO_2}/m^2/s[c]	D_{PtO_2}/m^2/s[d]	J_{CO_2}/molecules m^{-2}/s	z/mm	λ/mm[e]	J_{PtO_2}/molecules m^{-2}/s	J_{Pt}/μg cm^{-2}/min
500	2.3×10^{-6}	6.3×10^{-4}	1.4×10^{-3}	6.2×10^{-4}	2.4×10^{20}	53.2	3.5×10^{-3}	3.5×10^{15}	0.007
600	4.2×10^{-4}	3.6×10^{-3}	1.9×10^{-3}	8.4×10^{-4}	7.2×10^{21}	11.5	4.2×10^{-3}	5.8×10^{17}	1.2

[a] K_P values from Table 3

[b] Under conditions: $P_{CO} = 0.01$ bar and $P_{O_2} = 0.02$ bar

[c] For CO_2 in air [15] under experimental conditions

[d] For PtO_2 in air taking into account the ratio $D_{CO_2}/D_{PtO_2} = (M_{PtO_2}/M_{CO_2})^{1/2} = 2.27$

[e] $\lambda \approx 2.2 \times 10^{-10} T/P$ where P in bar [15]

Table 5 Literature values of the activation energies, E, reported for oxidation of CO on Pt catalysts

E/kJ/mol	T/K	Catalyst	Year	References
124	506–725	Pt wire	1922	[1]
56	>453	Pt/SiO_2	1978	[28]
104	300–700	Monolith	1982	[29]
100	400–450	Pt/SiO_2	1983	[30]
≈109	400–800	Pt/γ-Al_2O_3	1984	[31]
121	540–753	Monolith; 0.1 wt%Pt	1985	[32]
138	500–725	Pt(100) single crystal	1988	[33]
54	<440	Pt(100) single crystal		
101[a]	<473	Pt/γ-Al_2O_3	1991	[34]
83[b]	<473	Pt/γ-Al_2O_3		
≈53	323–430	Pt(111) single crystal	1993	[35]
125	560–770	Pt/α-Al_2O_3 (14 nm)[c]	1993	[36]
172	602–770	Pt/α-Al_2O_3 (1.7 nm)[c]		
94	443[d]	$2\%Pt/Al_2O_3$	1993	[37]
48	373[d]	$2\%Pt\text{-}14.7\%CeO_2/Al_2O_3$		
112	463–503	Pt/Al_2O_3	1997	[38]
71	423–523	Pt/γ-Al_2O_3	1997	[39]
78	423–623	Pt/Al_2O_3	2002	[40]
≈52	280–295	Pt(111) single crystal	2004	[41]
110	506[d]	Pt/γ-Al_2O_3	2004	[42]
132	513[d]	$Pt\text{-}CeO_2/\gamma\text{-}Al_2O_3$		
≈70	≈416[d]	$Pt\text{-}CeO_2$		
109	370–510	Pt nanoparticles stabilized by SiO_2 nanoparticles	2005	[43]
75	370–470	Pt/ZrO_2 (powdered)	2006	[44]
≈135	520–640	$Pt/ZrO_2/SiO_2$		
96	443–493	Pt/γ-Al_2O_3 (36 nm)[c]	2006	[45]
107	443–493	Pt/γ-Al_2O_3 (7 nm)[c]		
115	443–493	Pt/γ-Al_2O_3 (5 nm)[c]		
120	443–493	Pt/γ-Al_2O_3 (2 nm)[c]		
93	423–463	$Pt\text{–}Rh/\gamma$-Al_2O_3	2009	[46]
116	403–488	Pt/Al_2O_3	2010	[47]

[a] Without H_2

[b] With 1 vol% H_2

[c] Particle size

[d] The temperature at which 50% conversion is achieved

classical work by Langmuir in 1922 [1]. Taking together all 22 measurements (the sets of 9 and 13 points on the Arrhenius plot in [1]), the calculated magnitude of E is diminished from 133 to 124 kJ mol^{-1} [1].

Several conclusions can be deduced by comparative analyses of the data in Table 5. (i) Of the 31 values of E reported in 21 publications, 17 (more than half) are between 100 and 138 kJ mol^{-1}, giving the average magnitude: $E = 116 \pm 12$ kJ mol^{-1}. (ii) The (four) low values of E, between 48 and 54 kJ mol^{-1}, were obtained at temperatures below 400 K [33, 35, 37, 41]. A probable explanation for the increase of E values for reactions above 400 K is that CO_2 is desorbed from the reactor walls at these temperatures and, consequently, the reduction mode is transformed from equimolar ($P^{int}_{CO_2} > P^{ext}_{CO_2}$) at low temperatures to the isobaric regime ($P^{ext}_{CO_2} > P^{int}_{CO_2}$) (see above). The strong desorption of CO_2 from zeolites above 400 K has been confirmed experimentally [48]. Thus, it follows from the theory that the molar enthalpy of reaction, equivalent to the E parameter in the Arrhenius approach, should gradually increase by a factor of three. Thorough experiments by Berlowitz et al. [33] provide very satisfactory confirmation of this explanation.

Discussions of reported E values, having magnitudes between 100 and 138 kJ mol^{-1}, often identify this with the energy of CO desorption from Pt or with the formation of an activation complex for the reaction of CO with O, i.e., with an assumed transition state for the oxidation CO + ½ $O_2 \rightarrow CO_2$. No attempt to interpret the E value through thermochemical reasoning could be found in the literature, leaving the evaluation of the reaction enthalpy based on the novel mechanism described above, as the only application of this approach. It is of considerable interest, therefore, that agreement between the calculated value of molar enthalpy in the isobaric mode ($\Delta_r H^\circ_T/1 = 128$ kJ mol^{-1}) and the experimental magnitude of E, 116 kJ mol^{-1}, is very good. The discrepancy is within the limits of experimental and theoretical errors. Similarly, agreement between the calculated value of the molar enthalpy in the equimolar mode ($\Delta_r H^\circ_T/3 = 43$ kJ mol^{-1}) and the experimentally measured E value, 52 kJ mol^{-1}, is also highly satisfactory.

Reaction orders

From Eq. 24, it is expected that the rate of CO oxidation, J, is directly proportional to the partial pressure of Pt vapor, P_{Pt}, and, therefore:

$$J \propto K_P \times P^2_{CO}/P^2_{CO_2} \tag{30}$$

What can be deduced from this relationship? First, the CO oxidation rate is independent of oxygen partial pressure. Second, at constant CO partial pressure, the reaction rate J decreases with increase of CO_2 pressure. Third, when $P_{CO_2} \approx P_{CO}$, J is expected to be independent of changes in P_{CO}. From these relationships, it follows that at constant P_{CO_2} the oxidation rate dependence is described by the power function ($J \propto P^2_{CO}$). Thus, the exponent n in the power function $J \propto P^n_{CO}$ gradually changes from zero at $P_{CO_2} = P_{CO}$ to 2 with increasing P_{CO_2} up to $P_{CO_2} \gg P_{CO}$. When $P_{CO_2} \approx 2.5 P_{CO}$, $J \propto P_{CO}$.

Recent experimental studies by the Frenken group, applying the MvK mechanism [8, 49], confirm the first

conclusion (J is independent of oxygen pressure for CO oxidation over PtO_2). The effect of CO_2 in reducing the oxidation rate has also been confirmed experimentally. The article by Gülyüz et al. [50] is especially important here, by reporting that a two-fold increase of P_{CO_2} at constant values of $P_{CO} = 0.05$ bar and $P_{O_2} = 0.025$ bar reduces the oxidation rate by a factor of 3.5 (instead of the theoretical 4.0). This agreement is more than satisfactory.

Absolute rates of CO oxidation on Pt

Absolute rates of heterogeneous reactions, such as CO oxidation on Pt, are conventionally expressed either in molecules m^{-2} s^{-1} or as turnover frequencies (TOF) in molecules $site^{-1}$ s^{-1}. Platinum oxide has the trigonal crystallographic structure (IIIa): $a = b = 1.113$ Å, $c = 4.342$ Å, $\alpha = 60°$ giving the surface-area of a PtO_2 rhombus site as 8.39 $Å^2$ or approximately 1.2×10^{19} sites m^{-2}.

Probably, the first experimental measurements of the kinetics of CO oxidation on Pt wire were performed by Langmuir [1], who reported oxidation rates of ca. 1×10^{17} and 2×10^{19} molecules m^{-2} s^{-1} at 500 and 600 K, respectively. Sixty years later, Galwey et al. [51] undertook a similar study, using a constant flow reactant gas mixture (O_2/CO = 55/5), between 460 and 520 K and reported activation energy, E, values 150–210 kJ mol^{-1} and calculated pre-exponential factors, A, 10^{36}–10^{43} molecules m^{-2} s^{-1}. These give exponential factors at 490 K of 1.02×10^{-16} and 4.1×10^{-23} for $E = 150$ and 210 kJ mol^{-1}, from which J is found to be 1.0×10^{20} and 4.1×10^{20}, averaging 2×10^{20} molecules m^{-2} s^{-1} (within a factor of two). Scott et al. [52], working with a mixture of 20 mbar CO and 200 mbar O_2 in N_2 (300 cm^3 min^{-1}) determined the oxidation rate as $J = 4 \times 10^{22}$ molecules m^{-2} s^{-1} at 600 K. Ackermann et al. [49], working with a mixture of 80 mbar CO and 500 mbar O_2 at 625 K, determined the TOF number as 3×10^3 or $J = 3.6 \times 10^{22}$ molecules m^{-2} s^{-1}. Gao et al. [53] reported J values for low-vacuum experiments with $P_{CO} = 8$ mbar and $P_{O_2} = 16$ mbar at 500 and 600 K, as $J = 2.4 \times 10^{20}$ and 7.2×10^{21} molecules m^{-2} s^{-1}. It can be concluded from the above data that the averaged values of J (excepting Langmuir's results), correspond to about 10^{20}–10^{22} molecules m^{-2} s^{-1} in the range 500–600 K. However, the results reported recently by the Goodman group [53] are more reliable. These values have been used to estimate the boundary layer thickness, δ (see "Physical model" section above).

The retexturing effect

The changes of surface topography that accompany CO oxidation on Pt are well established. As early as 1922, Langmuir [2] noted: "Closer examination shows that the values for k (oxidation rate) tended to increase steadily, indicating that the filament was undergoing a progressive change in the direction of becoming a better catalyst… There is good evidence that the effect is caused by changes in the structure of the surface itself brought about by the reaction. After the wire has been used, the surface becomes very rough".

Systematic investigations of this effect were continued only in the mid-1970s. Galwey et al. [51, 52] described microscopic and kinetic observations of CO oxidation on Pt wires below 600 K and at atmospheric pressure. The heights of facets on platinum surface, developed during CO oxidation at ca. 500 K and measured from scanning electron micrographs, were in the range 0.1–1 μm. In contrast, Ackerman et al. [49] observed much smaller domain sizes, 7–20 nm.

We identify catalyst retexturing as resulting from the sequence of reactions involving (volatile) Pt species expressed by Eqs. 22 and 23:

$$PtO_2(s) \rightarrow Pt(g) \rightarrow PtO_2(g) \rightarrow PtO_2(s) \quad (31)$$

The most important steps that can impact on surface retexturing are those related to initial $PtO_2(s)$ reduction and subsequent $PtO_2(g)$ condensation. These steps are potentially capable of explaining the movement of metal at the surface resulting in catalyst retexturing. However, more detailed research on this process is required to understand precisely how "oxide movements" result in retexturing of the metal surface.

Conclusions

Application of concepts and theory recently applied successfully in the adjacent fields of heterogeneous reactions (thermal decompositions of solids and reduction of bulk oxides by gases) to the mechanistic analysis of experimental kinetic data reported in the literature, has resulted in the development of a new mechanism for the catalytic oxidation of CO on platinum through the PtO_2 intermediate**.** In place of the conventional MvK scheme, the two new reactions proposed are: $PtO_2(s) + 2CO \leftrightarrow Pt(g) + 2CO_2$and $Pt(g) + O_2 \leftrightarrow PtO_2(g) \rightarrow PtO_2(s)$. The first reaction determines the kinetics of CO oxidation and the second determines the kinetics of restoration of the PtO_2 layer. This oxidation mechanism confirms and develops the novel and challenging concept in heterogeneous catalysis that the solid is a chemically active participant in the reaction.

Thermochemical consideration of the kinetic features of the reaction, using the Langmuir quasi-equilibrium equations for the evaporation of simple substances has enabled

calculation of the reaction enthalpy, $\Delta_r H_T^\circ$, the equilibrium constant, K_P, and the absolute rate, J, of CO oxidation on platinum catalysts. Satisfactory agreement between these values, calculated theoretically and experimentally measured, confirms the validity of the new reaction model. (Calculations of these parameters are not possible using the Arrhenius model.) Furthermore, the thermochemical approach provides a quantitative interpretation of the strong effect of CO_2 in reducing the oxidation rate and the three-fold changes of the E parameter with temperature.

The authors believe that these new, and evidently more powerful, theoretical concepts used in the development of this novel mechanism of CO oxidation by PtO_2 are potentially applicable to a much wider range of heterogeneous catalytic reactions, in particular, kinetic and mechanistic interpretations of oxidation processes occurring with other reactants (H_2, CH_4, SO_2, etc.) and/or on other PGM catalysts (PdO, RuO_2, etc.).

References

1. Langmuir I. The mechanism of the catalytic action of platinum in the reactions $2CO + O_2 = 2CO_2$ and $2H_2 + O_2 = 2H_2O$. Trans Faraday Soc. 1922;17:621–54.
2. Langmuir I. Chemical reactions on surfaces. Trans Faraday Soc. 1922;17:607–20.
3. Taylor HS. A theory of the catalytic surface. Proc Roy Soc Ser A. 1925;108:105–11.
4. Hinshelwood CN. Kinetics of chemical change. Oxford: Clarendon Press; 1940.
5. Eley DD, Rideal EK. Parahydrogen conversion over tungsten. Nature. 1940;146:401–2.
6. IUPAC. Compendium of chemical terminology. 2nd Ed. Oxford: Blackwell; 1997.
7. Mars P, van Krevelen DW. Oxidations carried out by means of vanadium oxide catalysts. Spec Suppl to Chem Eng Sci. 1954;3:41–57.
8. Hendriksen BLM, Frenken JWM. CO-oxidation on Pt(110): scanning tunneling microscopy inside a high-pressure flow reactor. Phys Rev Lett. 2002;89: 046101–1-4.
9. L'vov BV, Ryabchuk GN. Studies of the mechanism of sample atomization in electrothermal atomic absorption spectrometry by analysis of absolute process rates: oxygen-containing compounds. Zh Analit Khim. 1981;36:2085–96. (in Russian).
10. L'vov BV, Fernandes GHA. Regularities in thermal dissociation of oxides in graphite furnace for atomic absorption analysis. Zh Analit Khim. 1984;39:221–31. (in Russian).
11. L'vov BV. The mechanism of the thermal decomposition of metal nitrates in graphite furnaces for atomic absorption analysis. Zh Anal Khim. 1990;45:2144–53. (in Russian).
12. L'vov BV. Mechanism of the thermal decomposition of metal nitrates from graphite furnace mass spectrometry studies. Mikrochim Acta (Wien). 1991;II:299–308.
13. L'vov BV, Novichikhin AV. Mechanism of thermal decomposition of anhydrous metal nitrates. Spectrochim Acta Part B. 1995;50:1427–48.
14. L'vov BV, Novichikhin AV. Mechanism of thermal decomposition of hydrated copper nitrate in vacuo. Spectrochim Acta Part B. 1995;50:1459–68.
15. L'vov BV. Thermal decomposition of solids and melts, new thermochemical approach to the mechanism, kinetics and methodology. Berlin: Springer; 2007.
16. L'vov BV. Fundamental restrictions of the second-law and Arrhenius plot methods used in the determination of reaction enthalpies in decomposition kinetics. J Therm Anal Calorim. 2008;92:639–42.
17. L'vov BV. Role of vapour oversaturation in the thermal decomposition of solids. J Therm Anal Calorim. 2009;96:321–30.
18. L'vov BV. Thermochemical approach to solid-state decomposition reactions against the background of traditional theories. J Therm Anal Calorim. 2009;96:487–93.
19. L'vov BV. Impact of the gaseous environment on the kinetics of solid-state decompositions. J Therm Anal Calorim. 2010;100:967–75.
20. L'vov BV. The mechanism of solid-state decompositions in a retrospective. J Therm Anal Calorim. 2010;101:1175–82.
21. L'vov BV, Galwey AK. The mechanism and kinetics of NiO reduction by hydrogen: thermochemical approach. J Therm Anal Calorim. doi:10.1007/s10973-011-2000-0.
22. Shumbera RB, Kan HH, Weaver JF. Oxidation of Pt(100)-hex-R0.7° by gas-phase oxygen atoms. Surf Sci. 2007;601:235–46.
23. Harano Y. The detection of atomic oxygen in the decomposition of some metallic oxides. Nippon Kagaku Zasshi. 1960;82:152–5. (in Japanese).
24. Ackermann MD. Operando SXRD: a new view on catalysis. Leiden: PhD Thesis. 2007. A digital version of this thesis is available at http://www.physics.leidenuniv.nl/sections/cm/ip.
25. Samsonov GV, editor. Physical–chemical properties of oxides. Reference book. Moscow: Metallurgiya; 1978. (in Russian).
26. Glushko VP, editor. Thermodynamic constants of individual substances. Reference book vol II book 2. Moscow: Nauka; 1979. (in Russian).
27. Schlichting H. Boundary-layer theory. 7th ed. New York: McGraw-Hill; 1979.
28. Cant NW, Hicks PC, Lennon BS. Steady-state oxidation of carbon monoxide over supported noble metals with particular reference to platinum. J Catal. 1978;54:372–83.
29. Oh SH, Cavendish JC. Transients of monolithic catalytic converters: response to step changes in feed stream temperature as related to controlling automobile emissions. Ind Engng Chem Prod Res Dev. 1982;21:29–37.
30. Herskowitz M, Kenny CN. Kinetics and multiple steady states. Can J Chem Engng. 1983;61:194–9.
31. Yu Yao Y-F. The oxidation of CO and hydrocarbons over noble metal catalysts. J Catal. 1984;87:152–62.
32. Subramaniam B, Varma A. Reaction kinetics on a commercial three-way catalyst: the CO–NO–O_2–H_2O system. Ind Engng Chem Prod Res Dev. 1985;24:512–6.
33. Berlowitz PJ, Peden CHF, Goodman DW. Kinetics of CO Oxidation on single-crystal Pd, Pt and Ir. J Phys Chem B. 1988;92:5213–21.
34. Muraki H, Matunaga S-I, Shinjoh H, Wainwright MS, Trimm DL. The effect of steam and hydrogen in promoting the oxidation of carbon monoxide over platinum on alumina catalyst. J Chem Tech Biotechnol. 1991;52:415–24.
35. Hardacre C, Ormerod RM, Lambert RM. Low-temperature carbon monoxide oxidation on Pt (111). Dependence of apparent activation energy on reactant gas composition. Chem Phys Lett. 1993;206:171–4.
36. Zafris GS, Gorte RJ. CO oxidation on Pt/α-Al_2O_3(0001): evidence for structure sensitivity. J Catal. 1993;140:418–23.
37. Serre C, Garin F, Belot G, Maire G. Reactivity of Pt/Al_2O_3 and Pt–CeO_2/Al_2O_3 catalysts for the oxidation of carbon monoxide by oxidation: II. Influence of the pretreatment step on the oxidation mechanism. J Catal. 1993;141:9–20.

38. Nibbelke RH, Campman MAJ, Hoebink JHBJ, Marin GB. Kinetic study of the CO oxidation over Pt/γ-Al_2O_3 and Pt/Rh/CeO_2/γ-Al_2O_3 in the presence of H_2O and CO_2. J Catal. 1997; 171:358–73.
39. Kahlich MJ, Gasteiger HA, Behm RJ. Kinetics of the selective CO oxidation in H_2-rich gas on Pt/Al_2O_3. J Catal. 1997;171: 93–105.
40. Kim DH, Lim MS. Kinetics of selective CO oxidation in hydrogen-rich mixtures on Pt/alumina catalysts. Appl Catal A General. 2002;224:27–38.
41. Burnett DJ, Capitano AT, Gabelnick AM, Marsh AL, Fischer DA, Gland JL. In situ soft X-ray studies of CO oxidation on the Pt(111) surface. Surf Sci. 2004;564:29–37.
42. Oran U, Uner D. Mechanisms of CO oxidation reaction and effect of chlorine ions on the CO oxidation reaction over Pt/CeO_2 and Pt/CeO_2/γ-Al_2O_3 catalysts. Appl Catal B Environ. 2004;54: 183–91.
43. Kapoor S, Belapurkar AD, Mittal JP, Mukherjee T. Catalytic oxidation of carbon monoxide over radiolytically prepared Pt nanoparticles supported on glass. Mater Res Bull. 2005;40: 1654–61.
44. Wootsch A, Descorme C, Rousselet S, Duprez D, Templier C. Carbon monoxide oxidation over well-defined Pt/ZrO_2 model catalysts: bridging the material gap. Appl Surf Sci. 2006;253: 1310–22.
45. Atalik B, Uner D. Structure sensitivity of selective CO oxidation over Pt/γ-Al_2O_3. J Catal. 2006;241:268–75.
46. Nikolaidis G, Baier T, Zapf R, Kolb G, Hessel V, Maier WF. Kinetic study of CO preferential oxidation over Pt-Rh/γ-Al_2O_3 catalyst in a micro-structured recycle reactor. Catal Today. 2009;145:90–100.
47. Liu L, Zhou F, Wang L, Qi X, Shi F, Deng Y. Low-temperature CO oxidation over supported Pt, Pd catalysts: particular role of FeOx support for oxygen supply during reactions. J Catal. 2010; 274:1–10.
48. Siriwardane RV, Ming-Shing Shen, Fisher EP. Adsorption of CO_2, N_2, and O_2 on natural zeolites. Energy Fuels. 2003;17: 571–6.
49. Ackermann MD, Pedersen TM, Hendriksen BLM, Robach O, Bobaru SC, Popa I, Quiros C, Kim H, Hammer B, Ferrer S, Frenken JWM. Structure and reactivity of surface oxides on Pt(110) during catalytic CO oxidation. Phys Rev Lett. 2005;95: 255505-1–4.
50. Gülyüz B, Aydinoğlu SO, Aksoylu AE, Önsan Zİ. Kinetics of CO oxidation over Pt-CeO_x supported on air-oxidized activated carbon. Turk J Chem. 2009;33:580–98.
51. Galwey AK, Gray P, Griffiths JF, Hasko SM. Surface retexturing of Pt wires during the catalytic oxidation of CO. Nature. 1985; 313:668–71.
52. Scott K, Griffiths JF, Galwey AK. Restructuring of catalyst surfaces during oscillatory reactions. In: Gray P, Nicolis G, Baras F, et al., editors. Spatial inhomogeneities and transient behaviour in chemical kinetics. Manchester: Manchester University Press; 1990. p. 579–92.
53. Gao F, Wang Y, Cai Y, Goodman DW. CO oxidation on Pt-group metals from ultrahigh vacuum to near atmospheric pressures. 2. Palladium and platinum. J Phys Chem C. 2009;113:174–81.